AIAA 98-0867
Hypersonic Boundary-Layer Transition for X-33 Phase II Vehicle

R. A. Thompson, H. H. Hamilton II, S. A. Berry, T. J. Horvath, and R. J. Nowak

NASA Langley Research Center
Hampton, VA 23681

36th Aerospace Sciences Meeting & Exhibit
January 12-15, 1998 / Reno, NV

HYPERSONIC BOUNDARY LAYER TRANSITION FOR X-33 PHASE II VEHICLE

Richard A. Thompson*, Harris H. Hamilton II†, Scott A. Berry*, Thomas J. Horvath*, Robert J. Nowak*

NASA Langley Research Center
Hampton, VA 23681-0001

Abstract

A status review of the experimental and computational work performed to support the X-33 program in the area of hypersonic boundary-layer transition is presented. Global transition fronts are visualized using thermographic phosphor measurements. Results are used to derive transition correlations for "smooth body" and discrete roughness data and a computational tool is developed to predict transition onset for X-33 using these results. The X-33 thermal protection system appears to be conservatively designed for transition effects based on these studies. Additional study is needed to address concerns related to surface waviness. A discussion of future test plans is included.

List of Symbols

h	heat-transfer coefficient, lbm/ft^2-sec $= q/(H_{aw}-H_w)$ where $H_{aw}=H_2$
h_{F-R}	reference heat-transfer coefficient from Fay-Ridell theory for sphere stagnation point
H	total enthalpy, BTU/lbm
k	roughness element height, inch
L	model reference length from nosetip, inch
M	freestream Mach number
q	heat transfer rate, BTU/ft^2-sec
Re	freestream unit Reynolds number, 1/ft
Re_θ	momentum thickness Reynolds number
x,y,z	Axial, lateral, and vertical distances, inch
α	angle of attack, deg
δ	boundary layer thickness, inch

Subscripts

aw	adiabatic wall condition
e	condition at local boundary layer edge
eff	effective
inc	incipient
tr	transition onset
w	surface condition
2	condition behind normal shock

Introduction

The X-33 program serves as a technology demonstration for development of a heavy-lift reusable launch vehicle (RLV).[1] In this capacity, the program should yield the basic technical and operational data to build and fly the RLV and insure its success. X-33 is envisioned as a one-half-scale prototype with full traceability of the design to the RLV. Consequently, the program faces critical design decisions of the nature expected for the full-scale RLV. Taken as a whole, the X-33/RLV program is fast-paced and ambitious project.

Following a Phase I competition for X-33, Lockheed-Martin Skunk Works was awarded the program to continue into Phase II and toward construction and flight of the vehicle. Rohr, Inc has primary responsibility for the thermal protection system (TPS) design as a subcontractor to Lockheed. The program is an industry-led effort in partnership with the U. S. Government in which NASA is tasked with supporting design and development of the vehicle through formal agreements. This paper covers a task agreement to study laminar-to-turbulent transition on the X-33 vehicle as part of that framework. It is best viewed as a work-in-progress since final design work on the X-33 remains to be completed. Results from studies completed as part of this task are included along with a discussion of ongoing efforts.

Transition Issues for X-33

Laminar-to-turbulent transition on any hypersonic vehicle influences the thermal protection system (TPS) and the allowable flight trajectories. As a result, vehicle weight, payload capacity, and mission are directly affected. Unfortunately, the uncertainty in predicting transition onset is often cause for overly conservative designs and reduced performance. This is a well-recognized problem that is no less evident for X-33. Also, because transition does not

---

* Aerospace Technologist, Aerothermodynamics Branch, Aero- and Gas-Dynamics Division.
† Aerospace Technologist, Aerothermodynamics Branch, Aero- and Gas-Dynamics Division. Associate Fellow AIAA.

scale with body size, the stated goal of traceability from X-33 to RLV cannot be absolutely achieved. At most, these transition studies can help design the vehicle at hand (i.e. the X-33) and help develop the techniques to apply to RLV. Transition effects on the TPS design and performance of RLV remain to be determined.

The onset of transition on any flight/reentry vehicle is dependent on factors such as body shape, surface roughness, and flight profile. Other less predictable effects (e.g., vibration, environment) can also play a role. A "zeroth-order" assessment of factors under the designers' control is useful to isolate problem areas and to direct focused studies. A discussion of these in relation to the current X-33 configuration follows.

Body shape

One distinguishing feature of the Lockheed X-33 vehicle (Fig. 1) is the "lifting body" shape. This blunt wedge-like vehicle resembles a class of slab-delta wings which have been widely studied over the last four decades. Many investigations have shown varying degrees of crossflow and significant movement of attachment lines over the windward surface depending on sweep angle and angle of attack. Both factors could play a role in transition on X-33. Although this vehicle shape has been maintained throughout development, it has evolved through several configurations to improve the aerodynamic design. The configurations pertinent to this work are listed in Table 1 along with a note of the major changes to the outer mold lines.

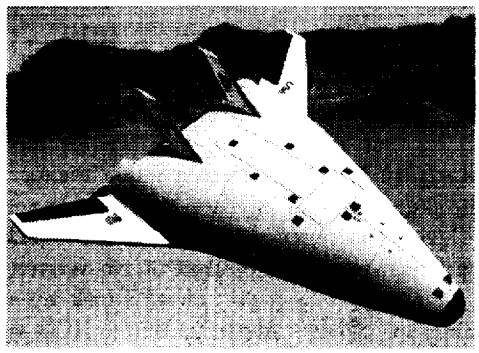

Figure 1. Lockheed X-33

Aerodynamic surfaces on the X-33 vehicle include canted fins, twin vertical tails, and dual body flaps for pitch/roll control. Elevons on the fins add additional lateral/pitch control. Deflection of any control surface is a likely source of windside transition due to the adverse pressure gradient and shock discontinuity introduced at the compression (for supersonic speeds). The likelihood of transition occurring on deflected body flaps and fin elevons led the X-33 designers to assume turbulent-level heating everywhere in these areas. Given this assumption, transition on control surfaces was excluded from this study.

Table 1. Lockheed X-33 configurations

Revision	Major Change
D-Loft	Configuration from Phase 1
Rev C	Changes in nose shape, 37° fin dihedral
Rev F	20° fin dihedral, larger body flaps, Rev C forebody

A similarity between the X-33 and Shuttle Orbiter exists in that both vehicles descend at angles of attack near 40 deg. Flowfields around each vehicle are dominated by the effectively blunt shape which gives rise to similar boundary-layer edge conditions on the windside (e.g., M_e between 1.5 and 2.0). Knowledge derived from Shuttle experience should prove useful for transition studies on X-33.

Surface

Advances in materials and structures have enabled Lockheed/Rohr to propose a unique system of composite metal panels over the windward surface for thermal protection. Panels vary in size depending on body location and are installed in an overlapping manner to eliminate inter-tile gaps and fillers. A sketch of the herringbone installation pattern of the panels on the windward surface is given in Fig. 2. A carbon composite is employed on the nose cap, fin leading edges, and elevators where the metallic TPS provides insufficient protection. Thermal protection of the wind-side body flaps is provided by ceramic tiles. The leeside surface is protected with an AFRSI blanket material.

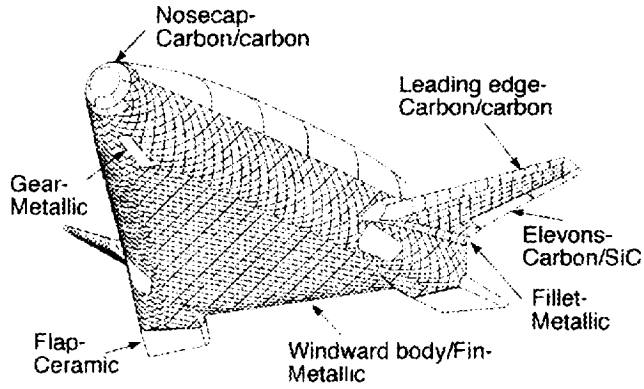

Figure 2. Windward surface TPS

Although the manufacturing and operational advantages of the X-33 TPS are substantial, these benefits must be measured against aerothermodynamic effects on transition and localized heating. Step discontinuities from a paneled (tiled) construction expose the flow to distributed roughness elements and potential adverse effects. Steps between adjoining materials and around doors introduce discrete roughness elements and the same concerns. Any single gap or step can trigger transition in the discrete sense, while the

distribution of discontinuities over the surface could produce transition through a compounding effect. The situation is very similar to a conventional ceramic tile system, such as used on Shuttle, where roughness dominates the transition process.

An additional effect on transition not present on Shuttle relates to thermal expansion of a metallic TPS that is apt to occur for X-33. Overlapping construction of the X-33 tiles allows for expansion; however, the rapid heating pulse associated with X-33 trajectories is predicted to produce bowing of the surface panels. The result is additional surface irregularities best characterized as a "wavy wall". The degree of bowing in the surface panels can vary over the surface and the trajectory depending on the tile exposure. Naturally, the panels most prone to bowing are in high heating regions near the nose and leading edges or chines.

A remaining area of concern for transition on the X-33 is the leeside flow. Large surface roughness and flow disturbances associated with vents and doors led Lockheed/Rohr to treat the leeside as fully turbulent for the TPS design. Thus, no study of leeside transition was undertaken in this work.

Trajectory

Flight requirements for a successful X-33 program are varied but include suborbital flights up to Mach 8 and Mach 15. During development, flight trajectories have changed with modifications of vehicle configuration and as constraints were met. However, the TPS design was based on the most severe of the early trajectories and has remained essentially fixed. This trajectory (designated "Malmstrom-4 (Old)") is illustrated in Fig. 3.

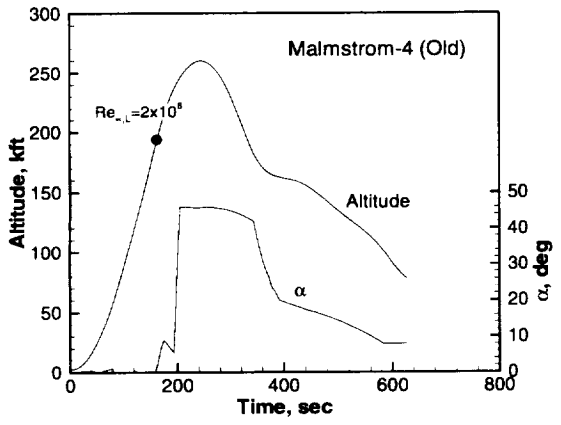

Figure 3. Malmstrom-4 (Old) trajectory

On ascent, the freestream Reynolds number based on vehicle length decreases to a value of 2×10^6 around 190,000 ft as shown in the figure. It is assumed that turbulent flow will prevail until this point. At higher altitudes (lower Reynolds number) the flow is assumed to laminarize and then transition back to turbulence during descent. During this phase, angle-of-attack ranges up 45 deg over a large portion of the trajectory. Heating rates on ascent are not predicted to reach a critical level; however, the reverse is true on descent. If transition of the windward surface boundary layer to turbulence occurs during the portion of the trajectory where peak heating is anticipated, then the increased heating would excede the TPS limits. The necessity to delay the onset of transition is obvious.

Approach

Since the design of a vehicle's shape, structure (TPS and weight), and flight trajectory are mutually dependent on flow transition and each other, an integrated process is preferred to achieve a final design. In practice this process is difficult to accomplish because it is time consuming and expensive, so the designer is faced with accepting assumptions to minimize lag in the design cycle. The problem is accentuated by the short-term, fast-paced nature of X-33. Nevertheless, a plan for including transition effects in the design cycle was developed as outlined below.

In assessing the TPS for X-33, a decision was made by Lockheed/Rohr to use a "worst case" trajectory for the TPS design with the knowledge that turbulent heating could be managed if it occurred below a certain Mach number and altitude range. Using the Malmstrom-4 (Old) trajectory (see Fig. 3) for this purpose, turbulence was assumed to occur below Mach 10 on descent. Since this design point was used as the basis for TPS sizing, a primary task was to verify that the assumption regarding transition onset was valid. To accomplish this task, the vehicle shape was assessed using the Re_θ/M_e correlation parameter to determine whether "natural" transition would occur below Mach 10, then an assessment of typical transition "by-pass" mechanisms such as roughness, waviness, etc. was undertaken. If these studies showed that transition onset was conservatively estimated, then margins could be established for the TPS design. If roughness or other mechanisms invalidated the original assumption on transition onset then the TPS design could not be "fixed" a priori and a means to incorporate the new transition information would be needed.

This later scenario is similar to the Shuttle experience where a minimum roughness could not be obtained and criteria to predict roughness-induced transition were required. Extensive wind tunnel testing and correlation of roughness effects (in terms of Re_θ/M_e vs. Re_k) were performed to establish this criteria for Shuttle.[2,3] Post flight analysis of Shuttle data have refined the correlation to make the models useful in regular operations.[4] Similar opportunities exist for X-33. In planned flight tests, the vehicle trajectories will start benign and gradually grow more severe as the flight envelope is expanded. Data obtained during flight will help develop the transition models further, thereby validating the design at each stage and creating more accurate models for operational use.

In summary, the design process followed by Lockheed/Rohr determined the approach taken in the present work. The specific steps needed were to determine the allowable roughness and assess whether other effects (e.g. waviness) invalidated the original estimate of transition onset. Development of a method to predict transition that could be coupled in the design cycle followed later. Details of the experimental and computational methods used to accomplish this work are given in the next two sections. Results of the experimental tests and computational analyses follow last with a discussion of the important findings.

Experimental Methods

Experiments for the present work were conducted in the NASA Langley Research Center (LaRC) 20-Inch Mach 6 Tunnel. The tunnel is a hypersonic blowdown facility that uses heated, dried, and filtered air as the test medium. Typical operating ranges for stagnation pressure are 30 to 500 psi, stagnation temperature from 760° R to 1000° R, and freestream unit Reynolds number from 0.5 to 8 million per foot. Nominal freestream Mach numbers range from 5.8 to 6.1. The tunnel has a 20.5 by 20-inch test section. Micol[5] provides a more detailed description of this facility, along with performance characteristics.

All measurements were performed using a two-color relative-intensity phosphor thermography technique to enable optical acquisition of the test data.[6,7,8] With this technique, silica ceramic wind-tunnel models are slip casted[9] and coated with a mixture of phosphors which fluoresce in two regions of the visible spectrum (red and green) when illuminated with ultraviolet light. The fluorescence intensity is dependent on the amount of incident light and local temperature of the phosphors. By acquiring fluorescence intensity images of an illuminated model exposed to the wind-tunnel flow, surface temperature maps can be calculated on portions of the model in the camera's view. A temperature calibration of the system conducted prior to the test provides the data needed to convert the two-color images to temperature. Acquiring images (temperatures) at different times in the wind-tunnel run enables local heat transfer to be computed. Comparisons of heat transfer measurements using conventional thin-film resistance gauges and the thermographic phosphor technique have shown excellent agreement.[10]

In routine use of this technique, the phosphor coating (~0.001 inch thick) has proven robust and does not typically require refurbishment between runs. This technique, which has been widely used at LaRC, offers two distinct advantages over conventional test methods. Foremost, the measurements provide a quantitative resolution of global temperatures and heating unlike discrete gauge measurements. In addition, the model construction, testing, and data reduction can be performed significantly faster and cheaper than other techniques allow. The global resolution and rapid testing this method allows were particularly important in the present work in order to study transition fronts on a complex three-dimensional vehicle in a timely and efficient manner.

Computational Methods

Computation of surface heating and flow properties for this work was performed using a coupled inviscid/boundary-layer technique. Comparison of surface heating predictions with experimental measurements is useful for assessing the flow state (laminar, transitional, or turbulent) while the flow properties are needed to compute the parameters used in transition correlations. Calculations were performed using the LAURA[11] and DPLUR[12] codes to provide the external inviscid flowfields. Surface properties were extracted from these solutions to provide conditions for the LATCH[13] (boundary-layer) calculations.

The LAURA (Langley Aerothermodynamic Upwind Relaxation Algorithm) code uses a finite-volume shock-capturing approach to solve high-speed viscous and inviscid flow problems. The algorithm incorporates a novel point-implicit relaxation scheme to obtain solutions efficiently on multi-processor computers. The code has been applied to a full range of hypersonic vehicles and flight conditions in routine use at LaRC. Like LAURA, the DPLUR (Data-Parallel Lower-Upper Relaxation) code is a finite-volume, shock-capturing algorithm for the steady-state solution of both inviscid and viscous flow fields on structured grids.

The LATCH (Langley Approximate Three-Dimensional Convective Heating) code uses an engineering technique to calculate heating on three-dimensional reentry vehicles. LATCH is based on the axisymmetric analog and uses approximate integral methods for general three-dimensional boundary layer results. It has been shown[13] to be in very good agreement with both experimental and Navier-Stokes results.

Results and Discussion

This section summarizes the results of the X-33 transition studies to date. Since a large number of tests were required, only selected data are presented to highlight the most important information. Table 2 summarizes the full range of experimental tests performed.

Table 2. Transition tests completed in the LaRC 20-Inch Mach 6 Tunnel

Revision	α, deg	Re x 10^{-6}/ft	Tests
D-Loft	20, 25,30 35, 40, 45	2.0-8.0	Smooth body
D-Loft	20, 30 40	0.5-6.0	Discrete roughness
Rev C	-5, 0 20,30,40	1.0-6.0	Leeside, yaw, smooth, fin trips

In the phosphor images presented herein, the color contours represent surface heat-transfer ratios inferred from the measured temperatures.[8] The ratios in each case are obtained by normalizing the experimental results by a stagnation-point value ($h_{f\text{-}R}$) computed using the Fay-Ridell relation[14] on a sphere with the model nose radius. On the contour scale, red colors indicate higher heating (temperatures) while the cooler surfaces tend toward blue.

For tests in the LaRC 20-Inch Mach 6 Tunnel, the ratio of surface temperature to total freestream temperature is approximately 0.6 for an uncooled model. Temperature ratios for the X-33 vehicle in flight range from 0.25–0.35 for conditions near Mach 10. This difference in temperature ratio is thought to have a small effect on the transition results. Unpublished data[15] obtained in the LaRC 15-Inch Mach 6 High Temperature Tunnel (with temperature ratios around 0.4) have shown no effect on transition when compared to test results from the LaRC 20-Inch Mach 6 using an identical test model. In addition, the computations for Shuttle in Ref. 2 showed that Re_θ/M_e at a given location was only slightly effected (~5%) by cooling for temperature ratios between 0.15 and 0.42. Similar trends are assumed for the present data.

Coupled LAURA-DPLUR/LATCH solutions are used in all cases to obtain the flow parameters needed for transition correlations. It should be noted that using coupled inviscid/boundary-layer solutions in this manner restricts application of correlations derived herein to similar methods. They should not be used with Navier-Stokes type solutions as these methods are known to give different boundary-layer edge properties. Appropriate models could be derived using those other methods to obtain the correlating parameters.

Smooth Body

Shortly after the X-33 Phase II program was awarded, an effort was initiated to map the transition behavior on the Lockheed concept. At the time, the most current configuration was the D-Loft and so a series of tests were designed to test this vehicle. Due to test section and Reynolds number constraints in the LaRC Mach 6 Tunnel a decision was made to build and test only the forward 70% of this configuration to maximize the likelihood of forebody transition. Ten-inch models were constructed on a 2.2% scale of the vehicle. The resulting shape included the entire vehicle forebody up to the root of the canted fin. With no afterbody/appendages and no applied surface roughness, this model was considered the baseline smooth body.

In the run matrix, freestream Reynolds number was varied from 2 x 10^6 to 8 x 10^6 /ft while angle of attack was varied from 20 to 40 deg (with one run at 45 deg). Thermographic phosphor images were obtained at each run condition to capture the global transition patterns. The results showed transition to move forward on the body with increasing Reynolds number; however, an unexpected behavior was observed with angle of attack. Figure 4 illustrates this behavior by comparing the images for angles of attack of 30- and 40-deg at a constant Re = 6 x 10^6/ft.

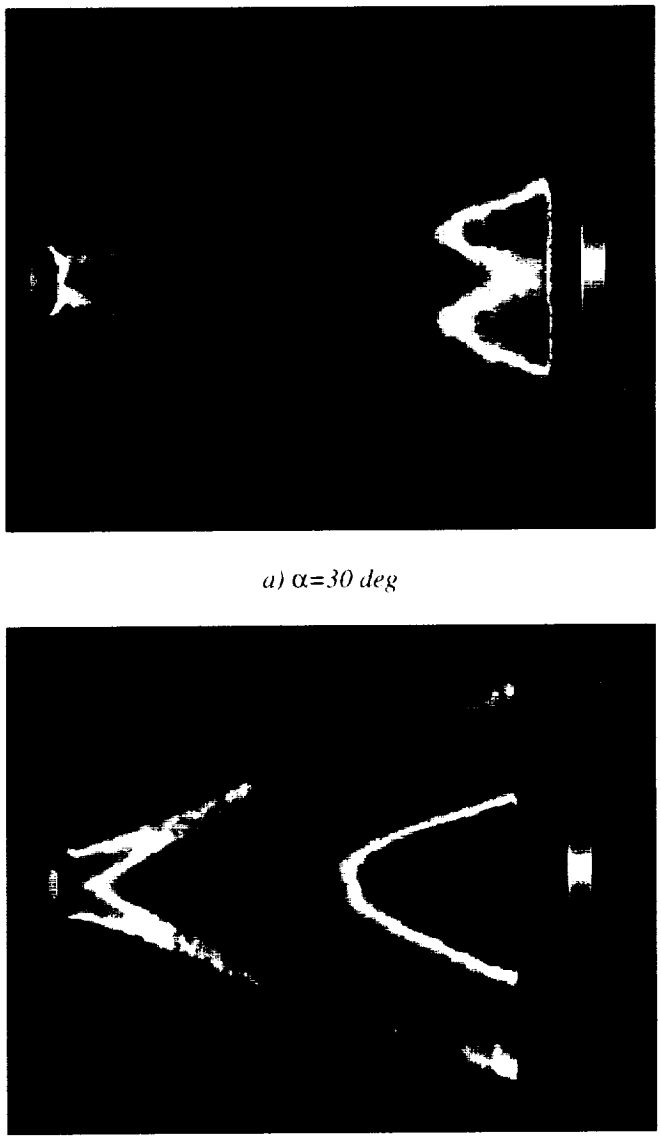

a) α=30 deg

b) α=40 deg

Figure 4. Effect of angle of attack on D-Loft "smooth" forebody transition for M=6 and Re=4x10^6/ft

A distinctive transition pattern with two lobes of high heating (one on each side of the centerline) is evident at the lower angle of attack. At 40 deg, the transition front appears as a single parabola shape symmetric about the centerline. Comparing images across the whole range of incidence showed a consistent trend. Namely, two transition fronts began outboard and coalesced into a single parabola shape as the angle of attack was increased. The existence of the two-lobed front is suggestive of a crossflow induced transition such as that examined on a swept wing in Ref. 16. Comparison of oil flow measurements in the present tests also supported a crossflow transition since inflow was seen

to occur at the lower angles of attack whereas the effect was relieved at higher incidence. Finally, using flowfield solutions from the LAURA code for the case at 30 deg to compute crossflow Reynolds numbers showed qualitative agreement with the location of the fronts although the computed values were not of the order typically reported (20-30 as compared to 200-250).

To obtain a smooth-body value of Re_θ/M_e for the X-33, computed contours of this ratio were compared against the experimental transition fronts. Results from the coupled inviscid (LAURA/DPLUR) and boundary-layer (LATCH) codes were used for this comparison. Contours of Re_θ/M_e on the forebody exhibited a parabolic shape similar to the transition front measured at high angles of attack which supported its use as a correlating factor. At low angles of attack, the computed Re_θ/M_e contours remained parabolic and did not predict a two-lobed front. This is not surprising because none of the parameters in the correlation could account for crossflow transition to a significant degree. In these cases, a parabolic fairing of the two-lobed front was used to give an average value.

Figure 5(a) illustrates how experimental transition points were extracted from the global image by using slices of the image data ("cut-lines") to produce normal heating plots. Transition onset was located at the point where heating departs from the laminar trend. Performing this procedure for a number of axial and longitudinal "cuts" yielded the discrete transition points shown in the figure. Matching these points with the computed contours shows agreement with a value of $Re_\theta/M_e = 300$ on the symmetry plane in this case (Fig. 5(b)). Applying this process to all test conditions yielded values between 250 and 325 as illustrated in Fig. 6. An average value of $Re_\theta/M_e \cong 285$ was chosen to represent this data and give a constant "smooth body" ratio. In comparison to the Shuttle, this ratio is larger than that established[2] using ground-based data (150-225) but is in agreement with recent tests on a smooth Shuttle model in the LaRC Mach 6 Tunnel.[17] The smaller Re_θ/M_e ratios obtained from previous ground-based Shuttle measurements have been attributed to noise disturbances in the tunnels which caused early transition on the aft end. The large Re_θ/M_e ratios in the present results suggest that noise may be less of a factor in these transition tests.

Roughness

The smooth-body transition criterion ($Re_\theta/M_e \cong 285$) provided an upper bound on the parameter since transition would tend to occur at lower values if roughness effects caused an earlier transition. For X-33, a value of Re_θ/M_e=250 was eventually chosen as the transition criterion based on a conservative view of the smooth-body ratio and experience from Shuttle. This number also agrees with the value that occurs for X-33 in flight at M=10 at a location where x/L=0.8 on the windward centerline. This is the same trajectory point where the flow was assumed to transition when the TPS was designed. To insure that transition

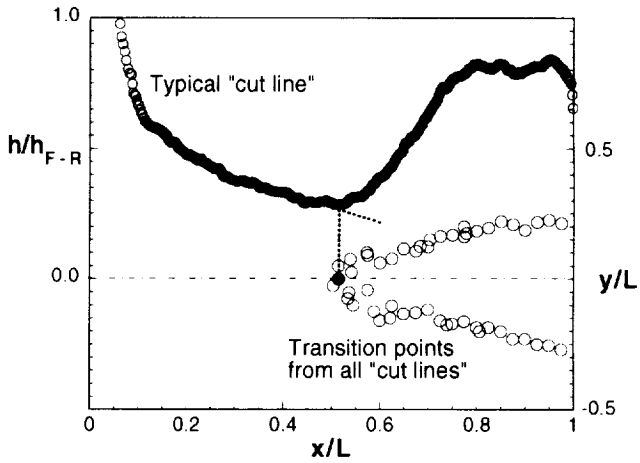

a) Extraction of experimental transition points

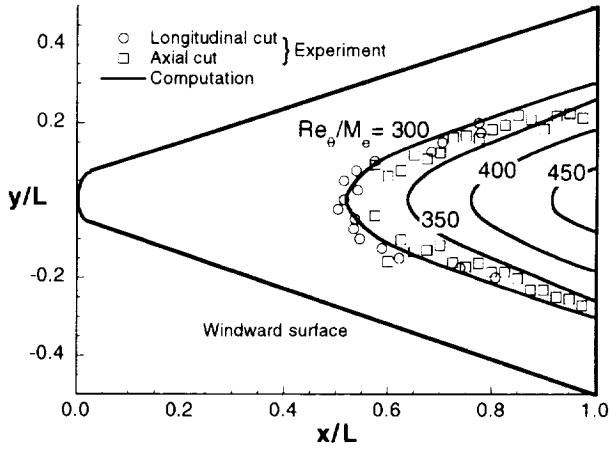

b) Correlation with computed Re_θ/M_e

Figure 5. Determination of "smooth body" value of Re_θ/M_e for M=6, α=40 deg, and Re=4x10^6/ft

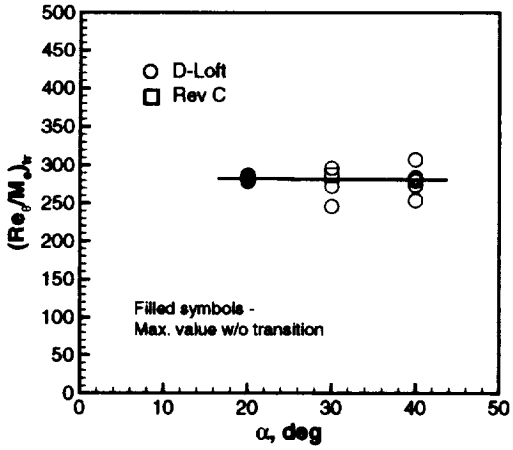

Figure 6. Smooth body transition correlation

would not occur earlier, a correlation between Re_θ/M_e and roughness was needed to determine a maximum roughness height.

Berry, et al.[17] presented a correlation of wind-tunnel data which related Re_θ/M_e with k/δ for isolated roughness elements on the Shuttle Orbiter. A similar approach was used to obtain a correlation for X-33 in the present study. The method described in Ref. 17 was to apply raised square patches of varying thickness at discrete surface locations to determine the "incipient" and "effective" transition Reynolds numbers. Transition was inferred using the phosphor thermography technique and an incipient value was found at the highest Reynolds number that maintained laminar flow. An effective value was determined at the minimum Reynolds where the transition front was fixed at the roughness element. Tunnel conditions were varied from run to run to locate the incipient and effective Reynolds numbers. Roughness elements were fabricated from 0.0025-inch Kapton tape which could be stacked in multiple layers to provide thickness variation. Tests with the Kapton tape showed it to be easily applied, non-detrimental to the phosphor coating, and robust to shear and heat stresses.

Figure 7 shows the locations of the discrete roughness elements on the X-33 model. Note that this is an identical 10-inch forebody model to that tested for the smooth body parameter. Five axial locations on the symmetry plane were selected for the trips (labeled A-E in the figure). The square tape elements were applied with a diagonal aligned with the symmetry plane (i.e., one corner facing forward) which has been shown to be the most effective orientation for tripping the boundary layer. Tests were performed with three roughness heights (0.0025, 0.005, and 0.0075-inch) at each of the five locations for 20, 30, and 40 deg angles of attack. A limited number of runs were made with trips at multiple stations and the total test matrix numbered 174 runs.

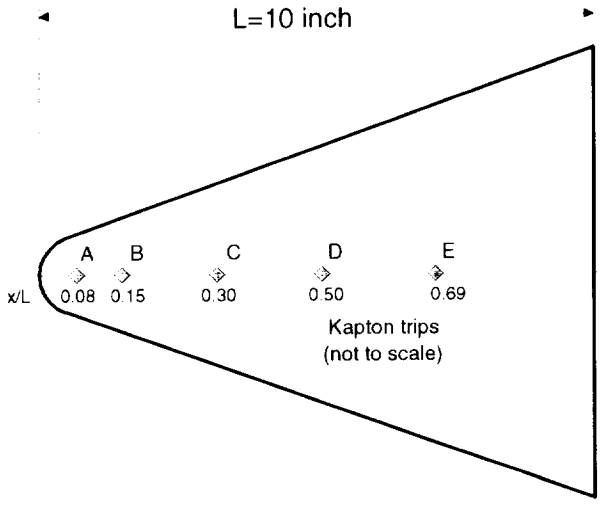

Figure 7. Forebody model for discrete roughness tests

A typical result from these tests for a single combination of trip height (0.005-inch), location (x/L=0.50), and angle of attack (40-deg) is presented in Fig. 8. The phosphor image shown in Fig. 8(a) illustrates transition at an effective Reynolds number and subsequent turbulent spreading due to the applied roughness in this case. The line plot shown in Fig. 8(b) gives the experimental heating rates along the symmetry plane for a range of Reynolds numbers.

a) Thermographic phosphor image for $Re=4.35x10^6$ /ft

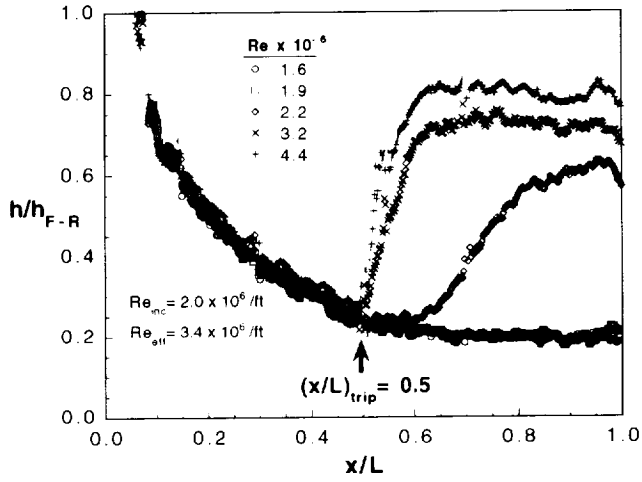

b) Centerline heat transfer rates

Figure 8. Results from discrete roughness test with k=0.005 inch at M=6, α=40 deg

This figure can be used to characterize the trip effectiveness for a given trip height as a function of Reynolds number. For example, at the two lowest Reynolds numbers, the trip is seen to have no effect on the downstream heating and the levels appear to remain laminar. At the next higher Reynolds number (2.2×10^6 /ft), the trip causes transitional heating of the downstream flow. Therefore, the incipient value lies between these two numbers (i.e. 1.9×10^6 /ft and 2.2×10^6 /ft). This intermediate value was determined by

assuming transition behaved similarly with Reynolds number for all trips having the same height. Comparing trends within this similar group provided a Reynolds number dependence that enabled an estimate of the exact value. An incipient Reynolds number of 2.0×10^6/ft was estimated for the case shown in Fig. 8. An effective Reynolds number of 3.4×10^6/ft was determined in a similar manner by searching for the condition which yielded fully turbulent flow just downstream of the trip. Incipient and effective Reynolds numbers for each combination of parameters (trip height, location, and angle of attack) were obtained following this procedure.

Computing Re_θ/M_e and boundary-layer thickness at each trip location for all effective and incipient Reynolds number pairs provided the necessary information to draw a correlation between transition and roughness. Figure 9 shows the resulting data which displays a generally well behaved trend in terms of Re_θ/M_e vs. k/δ. A correlation of the form $Re_\theta/M_e=C(k/\delta)^{-1}$, where C=45 for incipient and C=60 for effective, gives a conservative fit to the data. From this figure, flow conditions on the model remained laminar below the incipient curve, while above the effective curve the turbulent wedge was fixed at the roughness element.

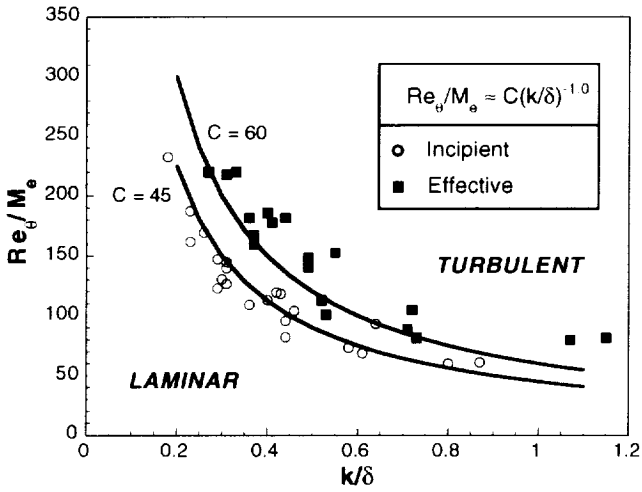

Figure 9. Roughness transition correlation

The incipient curve shown in Fig. 9 provided a basis for determining allowable roughness heights on the X-33. The maximum roughness height was fixed by choosing a ratio of Re_θ/M_e where transition is assumed to occur and computing the boundary layer thickness to determine k. Roughness height less than the maximum should be negligible while larger values begin to cause transition Using the X-33 criterion (Re_θ/M_e=250) in this manner gave $k/\delta = 0.2$. Applying this constraint to the calculated boundary layer at the Mach 10 design point yielded the allowable heights shown in Fig. 10. Comparison of the allowable heights to the manufacturing tolerances on X-33 revealed that the roughness constraints were easily met (except possibly near the fin root). Therefore, it appeared that roughness effects would not invalidate the transition criterion and transition estimates used in the TPS design were conservative.

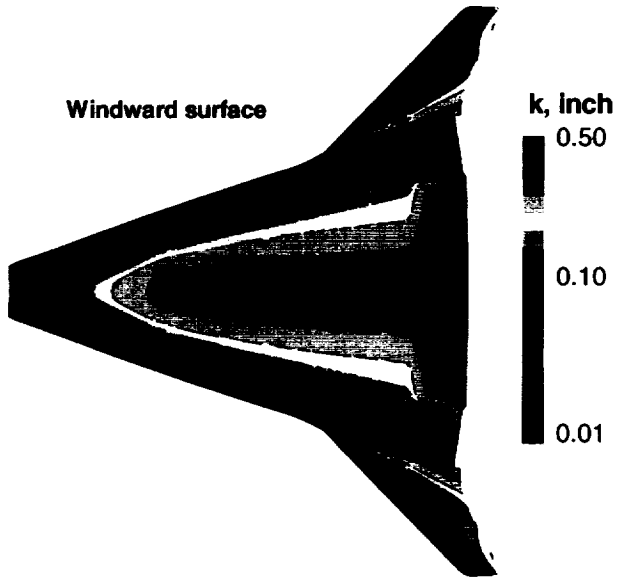

Figure 10. Allowable roughness heights on windside for $(Re_\theta/M_e)_{tr} = 250$

Full Body Tests

Because the smooth- and rough-body investigations were limited to the forebody, thermographic phosphor tests for the full vehicle (forebody, fins, body flaps) were performed on a 10-inch 1.32% scale model of the Rev C configuration. The possibility of early transition on the fins (relative to the body) and the general effects of yaw and body flap deflections were concerns to be addressed. A select number of tests (~50) were completed to investigate these issues for the conditions shown in Table 2.

Although some differences in nose shape exist between the D-Loft and Rev C configurations, the baseline (smooth-body) transition for the Rev C models was found to occur at the same length Reynolds numbers. This corresponds to a location further aft on the vehicle compared to the previous experiments due to the smaller scale. Matching transition front with computed values of Re_θ/M_e on the Rev C model indicated a smooth-body ratio of 285 as shown in Fig. 6 for the test at α=30 deg. This is in agreement with the smooth forebody result discussed previously for the larger D-Loft model. However, some evidence was found to suggest that body flap deflections served to damp transition when it occurred near the vehicle aft end. More detailed study is needed to quantify this effect and better determine the afterbody influence (if any). Additional tests of the baseline model at 30-deg angle of attack and 2-deg yaw showed only slight asymmetry of the surface heating and no adverse affect of the sideslip on transition for Reynolds numbers up to 6×10^6/ft. In all, none of the effects from this set of results showed significant differences with previous tests.

Regions on and around the canted fin were of concern for the TPS because large roughness due to steps between panels is expected in the area. Also, at hypersonic speeds the vehicle's bow shock lies close to the surface and interacts with the protruding fins. Strong bow-shock/wing-shock interaction would be expected to introduce transition on both the fin surface and leading-edge attachment line. This occurs on the Shuttle Orbiter near midspan and is thought to cause transition to appear first on the outboard wing surface.[18] Smooth-body tests with the full configuration indicated that transition would begin on the windward centerline prior to the fin for all conditions tested. Thus, early transition on the fin does not appear a problem for the smooth body.

To assess roughness effects on the fin, a set of qualitative tests were performed with discrete roughness elements (Kapton tape) applied at the location of expected joints and gaps in the wing root and leading edge. Figure 11 shows the location of these elements on the model. Tests at Reynolds numbers from 1 x 10^6 to 4 x 10^6 /ft and angles of attack of 20- and 30-deg were performed. Trip heights of 0.075 inch were tested at locations numbered 1, 5, and 8, individually and simultaneously. An additional trip with the same height was placed on the windward centerline at the 30% station to obtain a relative comparison.

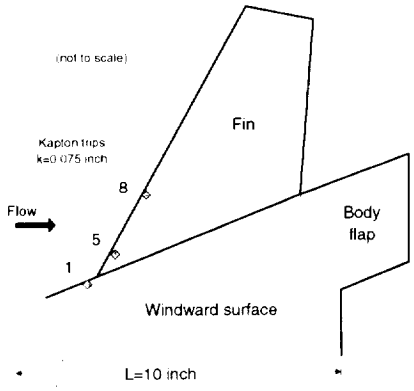

Figure 11. Discrete roughness elements on fin

Fig. 12 shows a full body phosphor image for a test at 30-deg angle of attack and Re=4.4 x 10^6 /ft with all three trips applied. This result is typical of all measurements made during that series of runs. None of the cases showed high heating evenly distributed over the fin which might indicate rapid transition along the attachment line due to the roughness. At most, the roughness produced heating "streaks" behind the elements as shown in the figure. In contrast, the roughness element on the vehicle forebody consistently acted as an effective trip during the same run. From these qualitative measurements, it appears that the fin region is no more sensitive to roughness than the forebody.

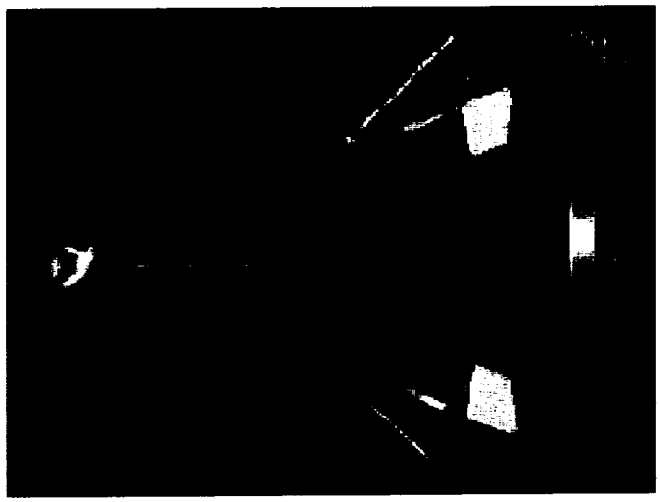

Figure 12. Thermographic phosphor image with roughness on fin at M=6, α=30 deg, Re=4.4x10^6/ft

Bowed Panel and Future Tests

As discussed in the introduction, bowing of the TPS panels is predicted to occur during the descent period and a potential exists for the resulting "wavy wall" to promote early transition. This occurrence has not been accounted for in the TPS design and is a significant open question. Tests to establish the importance of panel bowing for X-33 are planned, but no results are currently available. In preliminary efforts, several wind tunnel models incorporating an array of bowed panels of various heights were constructed. An 80-deg slab-delta wing geometry was used to address model design issues and demonstrate fabrication techniques associated with a "wavy wall". A rapid prototyping technique was used to build resin stereolithography (SLA) models which served as patterns to cast the actual ceramic wind tunnel models. It was demonstrated that panel heights down to 0.003-inch could be successfully captured on the model surface without resorting to more conventional machining techniques. The resulting bowed-panel ceramic models possessed some degree of surface roughness inherent to the SLA technique. No attempt was made to eliminate the roughness for that test series. Results from that preliminary investigation clearly showed the wavy surface introducing disturbances into the flowfield. While no conclusions related to X-33 could be drawn, those tests did reinforce the need to assess this effect.

In designing the bowed-panel experiments for X-33, three panel heights were selected for study: 0.002, 0.004, and 0.006-inch. The smallest height is approximately in geometric proportion between the wind-tunnel model and full-scale vehicle. The ratio of panel height to boundary-layer thickness is also approximately matched between the wind-tunnel and a flight condition near Mach 10. Placement of surface panels on the model is designed to simulate areas where the most severe bowing is expected. In the test plan,

three sets of panels located in the nose and forward chine region will be tested individually and simultaneously in an effort to better understand any effects that might be measured. At present, the X-33 resin models with the bowed panel arrays have been constructed. Efforts to eliminate the roughness associated with the SLA technique have been successful for these models. Analysis of the experimental data will likely follow the procedure used by Goodrich, et al.[3] to correlate distributed roughness tests on Shuttle.

In future testing, the smooth body, roughness, and full body studies will be repeated using the Rev F configuration to assess changes from the D-Loft and Rev C vehicle. Initial screening will be done to determine the extent that the shape changes alter the results obtained previously and all tests will be repeated if necessary.

Transition Function

The experimental transition work presented in this paper has supported the use of an Re_θ/M_e criterion to predict transition onset for X-33. The simplicity of this result has enabled development of a numerical tool which predicts whether transition occurs at a station on the windward centerline for a given altitude, velocity, and angle-of-attack condition. Coupling this tool with trajectory simulations should enable modifications of the flight profile to be made while still honoring the transition and TPS design constraints. Conservatism in the design could be assessed and possibly reduced as a result.

The transition tool is based on a database of numerical simulations which cover the range of freestream and angle of attack values expected during flight. For X-33, a domain was selected where altitude ranged from 30 to 80 km for freestream velocities between 1 and 5 km/s and angles of attack between 0 and 40 deg. A total of 275 flow solutions were computed for discrete combinations of these parameters. Each calculation was done using the LATCH code to provide a distribution of Re_θ/M_e along the windward centerline. Since LATCH requires edge properties from a full flowfield solution, it was necessary to make an approximation for the approach to be tractable. This was done using a single inviscid flowfield solution from LAURA or DPLUR at each angle of attack for all altitudes and velocities. This approximation is valid for all altitudes since the inviscid solution is independent except when real gas effects are important. It is valid for all velocities if the Mach number is large (~10 or greater) since the shock shape and normalized pressure distributions are nearly invariant. To extend the validity for X-33, the inviscid solutions between 20- and 40-deg angle of attack were done for Mach numbers around 10 and around 6 for angles between 0 and 15 deg. Real gas effects were included by doing equilibrium air calculations at the high Mach number and perfect gas at Mach 6. It should be noted that these inviscid solutions are tailored to the design trajectory. Solutions at different conditions (e.g. low Mach number at high angle of attack) could cause inaccurate results for large dispersions.

A numerical function that uses the database of solutions was developed to provide the final transition tool. The function was derived by simple interpolation of the data to locate the altitude that transition occurs at a specified body point for all combinations of velocity and angle of attack. Figure 13 shows the function using the X-33 transition criterion (Re_θ/M_e=250) and a point at x/L=0.8. The result is a fairly planar three-dimensional surface which separates laminar flow above from transitional/turbulent flow below.

In practice, the function can be used to signal transition by plotting a trajectory in this space and locating the point

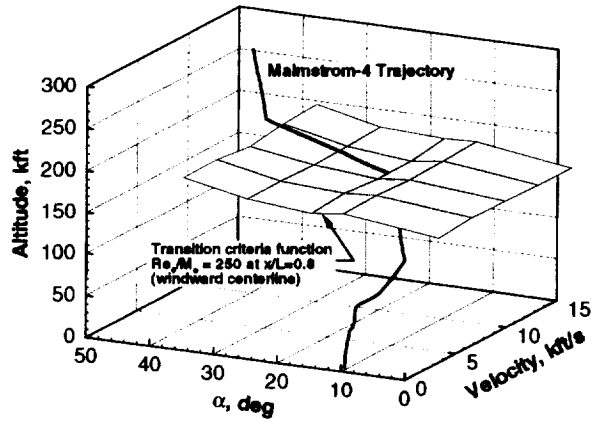

Figure 13. Transition surface

where it pierces the surface as shown in the figure. A computer routine that returns this intersection point was developed for integration with trajectory simulations. Families of surfaces have been generated by choosing different values of Re_θ/M_e and transition movement (based on the criterion) has been predicted by using different body points in the interpolation.

Summary

Wind tunnel tests have shown that a correlation based on Re_θ/M_e predicts the smooth body transition on the X-33 forebody. A constant value of $Re_\theta/M_e \cong 285$ was derived from this work. To accommodate roughness, a series of tests were used to correlate Re_θ/M_e with roughness height (k/δ). A final value of $Re_\theta/M_e = 250$ was chosen as the transition criteria for X-33 based on the smooth body tests and Shuttle experience. This value also matches the ratio expected to occur in flight at the point where transition was assumed when the TPS was designed. Given this trajectory point and the correlation, an allowable roughness over the vehicle was determined.

The roughness of the actual vehicle is expected to fall below the allowable values except in the wing root and

leading edge region; however, qualitative tests of large roughness in those regions did not reveal cause for concern. Thus, the transition point assumed for design of the TPS appears to be conservative for the tests performed to date.

Additional tests to determine the effect of distributed roughness due to a "wavy wall" from bowing of the TPS panels are planned. This effect is a major unanswered question at present. Repeat tests of the smooth body and discrete roughness models are also planned using the latest vehicle configuration. A final assessment of transition on X-33 awaits the completion of these tests.

Based on the smooth body and discrete roughness results, a numerical function was developed to provide a simple transition criterion for X-33. The function is useful for additional system studies and should enable the designer to further tailor the TPS and trajectory design.

Acknowledgment

The authors would like to thank the following people for contributions to this work: Mark Cagle, Mike Powers, Mark Griffith, Grace Gleason, Rhonda Manis, Johnny Ellis, Bert Senter, Glen Bittner, Ron Merski, and Lisa Brilliant.

References

[1] Freeman, D. C., Talay, T. A., and Austin, R. E, "Reusable Launch Vehicle Technology Program," AIAA Paper IAF 96-V.4.01, October 1996.

[2] Bertin, J. J., Hayden, T. E., and Goodrich, W. D., "Shuttle Boundary-Layer Transition Due to Distributed Roughness and Surface Cooling," Journal of Spacecraft and Rockets, Vol. 7, No. 3, Sep-Oct 1983, pp.389-396.

[3] Goodrich, W. D., Derry, S. M., and Bertin, J. J., "Shuttle Orbiter Boundary Layer Transition at Flight and Wind Tunnel Conditions," in Shuttle Performance: Lessons Learned: Part 2, Arrington, J. A. and Jones, J. J., ed., NASA CP-2283, pp. 753-779

[4] Bouslog, S. A., An, M. Y., and Derry, S. M., "Orbiter Windward-Surface Boundary-Layer Transition Flight Data," in Orbiter Experiment (OEX) Aerothermodynamic Symposium: Part 2, Throckmorton, D. A., ed., NASA CP-3248, pp. 703-740.

[5] Micol, J. R., "Hypersonic Aerodynamic/Aerothermodynamic Testing Capabilities at Langley Research Center: Aerothermodynamic Facilities Complex," AIAA Paper 95-2107, June 1995.

[6] Buck, G. M., "Automated Thermal Mapping Techniques Using Chromatic Image Analysis," NASA TM 101554, April 1989.

[7] Buck, G. M., "Surface Temperature/Heat Transfer Measurement Using a Quantitative Phosphor Thermography System," AIAA Paper 91-0064, January, 1991.

[8] Merski, N. R., "Reduction and Analysis of Phosphor Thermography Data with the IHEAT Software Package," AIAA Paper 98-0712, January, 1998.

[9] Buck, G. M. and Vasquez, P., "An Investment Ceramic Slip-Casting Technique for Net-Form, Precision, Detailed Casting of Ceramic Models," U.S. Patent 5,266,252, November 30, 1993.

[10] Micol, J. R., "Aerothermodynamic Measurement and Prediction for a Modified Orbiter at Mach 6 and 10 in Air," AIAA Paper 91-1436, June 1991.

[11] Cheatwood, F. M. and Gnoffo, P. A., "Users Manual for the Langley Aerothermodynamic Upwind Relaxation Algorithm (LAURA)," NASA TM-4674, April 1996.

[12] Candler, G. V., Wright, M. J., and McDonald, J. D., "Data Parallel Lower-Upper Relaxation Method for Reacting Flows," *AIAA Journal*, Vol. 32, No. 12, December 1994, pp. 2380-2386.

[13] Hamilton II, H. H., Greene, F. A., and DeJarnette, F. R., "Approximate Method for Calculating Heating Rates on Three-Dimensional Vehicles," *Journal of Spacecraft and Rockets*, Vol. 31, No. 3, May-June 1994, pp. 345-354.

[14] Fay, J. A. and Ridell, F. R., "Theory of Stagnation Point Heat Transfer in Dissociated Air," *Journal of Aeronautical Sciences*, Vol. 15, No. 2, 1958.

[15] Merski, R. N. Private communication.

[16] Cattafesta III, L. N., Iyer, V., Masad, J. A., King, R. A., and Dagenhart, J. R., "Three-Dimensional Boundary-Layer Transition on a Swept Wing at Mach 3.5," *AIAA Journal*, Vol. 33, No. 11, November 1995, pp. 2032-2037.

[17] Berry, S. A., Bouslog, S. A., Brauckmann, G. J., and Caram, J. M., "Boundary Layer Transition Due to Isolated Roughness: Shuttle Results from the LaRC 20-Inch Mach 6 Tunnel," AIAA Paper 97-0273, January 1997.

[18] Hartung, L. C. and Throckmorton, D. A., "Computer Graphic Visualization of Orbiter Lower Surface Boundary-Layer Transition," AIAA Paper 84-0228, 1984.